

Stimulating and toxic effect of chromium on growth and photosynthesis of a marine chlorophyte

Qiong Zhang^{1,2,3} , Philip D. Charles⁴ , El Mahdi Bendif^{3,5} , Svenja S. Hester⁴, Shabaz Mohammad⁴  and Rosalind E. M. Rickaby³ 

¹Department of Ocean Science and Center for Ocean Research in Hong Kong and Macau (CORE), The Hong Kong University of Science and Technology, Clear Water Bay, Hong Kong SAR, 999077, China; ²Southern Marine Science and Engineering Guangdong Laboratory (Zhuhai), Tang Qi Road, Zhuhai, 519000, China; ³Department of Earth Sciences, University of Oxford, South Parks Road, Oxford, OX1 3AN, UK; ⁴Department of Biochemistry, University of Oxford, South Parks Road, Oxford, OX1 3QU, UK; ⁵Institut des sciences de la mer de Rimouski (ISMER), Université du Québec à Rimouski, Rimouski, G5L 3A1, QC, Canada

Author for correspondence:

Qiong Zhang

Email: qiongz@ust.hk

Received: 6 August 2023

Accepted: 9 October 2023

New Phytologist (2024) 241: 676–686

doi: 10.1111/nph.19376

Key words: chromium, photosynthesis, phytoplankton, proteomics, trace metal.

Summary

- Marine phytoplankton can interchange trace metals in various biochemical functions, particularly under metal-limiting conditions. Here, we investigate the stimulating and toxicity effect of chromium (Cr) on a marine Chlorophyceae *Osetreococcus tauri* under Fe-replete and Fe-deficient conditions.
- We determined the growth, photosynthesis, and proteome expressions of *Osetreococcus tauri* cultured under different Cr and Fe concentrations.
- In Fe-replete conditions, the presence of Cr(VI) stimulated significantly the growth rate and the maximum yield of photochemistry of photosystem II (F_v/F_m) of the phytoplankton, while the functional absorption cross-section of photosystem II (σ_{PSII}) did not change. Minor additions of Cr(VI) partially rescued phytoplankton growth under Fe-limited conditions. Proteomic analysis of this alga grown in Fe-replete normal and Fe-replete with Cr addition media (10 μ M Cr) showed that the presence of Cr significantly decreased the expression of phosphate-transporting proteins and photosynthetic proteins, while increasing the expression of proteins related to carbon assimilation.
- Cr can stimulate the growth and photosynthesis of *O. tauri*, but the effects are dependent on both the Cr(VI) concentration and the availability of Fe. The proteomic results further suggest that Cr(VI) addition might significantly increase starch production and carbon fixation.

Introduction

Chromium (Cr) is widely used in industries for corrosion inhibition, electroplating, paints, pigment manufacturing, and leather tanning, and can be released to the environment from these anthropogenic sources (Richard & Bourg, 1991). Chromium also occurs naturally in aqueous environments by weathering and leaching of rocks (Rudnick & Gao, 2003). Release of Cr to natural waterways from crushed basalt rocks could be accelerated by enhanced weathering approaches that have shown great potential for removing CO₂ and stabilising climate (Taylor *et al.*, 2016; Beerling *et al.*, 2020). In aquatic systems, Cr concentrations are reported to range between 0.1 and 500 μ g l⁻¹ (2 nmol l⁻¹–10 μ mol l⁻¹; Jeandel & Minster, 1987; Cervantes, 2001; Wilson *et al.*, 2019). Hexavalent and trivalent forms are the most common and stable species of Cr in natural environments (Richard & Bourg, 1991), in which Cr(VI) has very high solubility and bioavailability under toxic conditions (Zhang *et al.*, 2018a, 2019a,b). When Cr(VI) enters into cells, it reacts spontaneously with the intracellular reductants and generates short-lived

intermediates Cr(V) and/or Cr(IV) that can be ultimately converted to Cr(III) in cells (Viti *et al.*, 2014; Zhang *et al.*, 2019a,b; Marković *et al.*, 2022). In the cytoplasm, some of the Cr(V) that is generated can be re-oxidised to Cr(VI) producing reactive oxygen species (ROS; Cheung & Gu, 2007). Reactive oxygen species can easily combine with DNA–protein complexes and induce oxidative stress in cells, including DNA damage, gene mutation, sister chromatid exchange, chromosomal aberrations, cell transformation, and dominant lethal mutation in a number of targets in cells. Although short-lived, Cr(IV) is able to bind to intracellular components (e.g. DNA–protein complexes), altering their physiological function (Cheung & Gu, 2007). Until now, little is known about Cr speciation, metabolism, and whether Cr may have a biological function in cells more generally.

Phytoplankton are at the base of the food chain in aquatic ecosystems and are responsible for the vast majority of primary production in the ocean. Through photosynthesis, they produce half of the oxygen in the air, and fix carbon which sinks into the deep ocean. The growth of phytoplankton may be largely affected by their living environment (Zhang *et al.*, 2022). Due to ideas of

climate mitigation by enhanced weathering strategies using basalt, which has very high levels of Cr (Rudnick & Gao, 2003; Flipkens *et al.*, 2021), there may be an unanticipated consequence of input of Cr into the rivers and ocean, causing an increase in Cr concentrations in the marine environment. Therefore, understanding phytoplankton response to Cr is becoming even more timely in recent years. Although there has been no confirmed biological function of Cr(III) or Cr(VI) in phytoplankton (Aharchaou *et al.*, 2017), a significant difference has been found in the uptake strategies and storage of Cr between the red (containing chlorophyll *a* + *b*) and the green (containing chlorophyll *a* + *c*) algal lineages (Zhang *et al.*, 2018b; Wilson *et al.*, 2019). These two groups of phytoplankton also display different susceptibilities to Cr toxicity (Wilson *et al.*, 2019). The green lineages of phytoplankton appear to have a higher tolerance to Cr toxicity (Wilson *et al.*, 2019). Although most previous studies focus on the toxicity of Cr, within this preliminary data, there was a hint that Cr might stimulate the growth of some marine phytoplankton species (Wilson *et al.*, 2019), but such effects were not investigated in detail. It is unclear whether Cr may substitute into some proteins that have certain metabolic functions in phytoplankton, similar to the chemical behaviour of Cd, which can substitute for Zn in some forms of carbonic anhydrase (Price & Morel, 1990). Here, based on previously published data, we further explore the physiological impacts and potential benefits of Cr elevated beyond typical surface open ocean concentrations (*c.* 2.4 nmol l⁻¹; Goring-Harford *et al.*, 2018) on a cosmopolitan marine Chlorophyceae *Ostreococcus tauri* (Belevich *et al.*, 2021; Yung *et al.*, 2022), by investigating their photosynthesis associated parameters, metallomes, and expressed proteomes.

Materials and Methods

Growth experiments

The microalgal strain *Ostreococcus tauri* Courties et Chrétiennot-Dinet used in this study was kindly provided by Dr Gwenael Piganeau (UMR7232 BIOM, Sorbonne-Universités, CNRS, France). All other phytoplankton were obtained from Roscoff Culture Collection (Roscoff, France) and were cultured in Aquil* medium (Morel *et al.*, 1979; Wilson *et al.*, 2019). The *Ostreococcus* cells were cultured in Aquil* medium containing 100 µM EDTA (Morel *et al.*, 1979; Wilson *et al.*, 2019) but with modified Fe and Cr concentrations. We performed growth experiments on the strain under both Fe-replete (1 µM total Fe) and Fe-deficient (0.1 µM total Fe) conditions. Fe was added in the form of FeCl₃. The concentrations of different species of Fe and Cr were estimated using VisualMinteq. The parameters were set to the experimental conditions of 17°C and pH = 8.1. The concentrations of all compositions of the medium were following Aquil* recipes with modified Fe and Cr concentrations. For all the experiments, the phytoplankton were cultured in acid-clean sterile plastic culture flasks. The blanks of Cr for the culture flask were analysed and determined to be below the detection limits (0.03 ng ml⁻¹, *c.* 0.6 nM l⁻¹) of inductively coupled plasma-mass spectrometry (ICP-MS) following the previously published

work (Zhang *et al.*, 2018b). The change in other trace-metal concentrations in the growth medium was negligible after the addition of Cr, based on ICP-MS measurement.

For growth experiment under Fe-replete condition, the growth medium used was Aquil in the control group (Sunda *et al.*, 2005) and modified by adding 10 µM l⁻¹ Cr(VI) in the form of K₂Cr₂O₇ in the Cr-treated group (Wilson *et al.*, 2019). This concentration is representative of the high end of the scale of Cr concentration found in the environment (e.g. Irajá River estuary; Pfeiffer *et al.*, 1982), although in most natural waters, Cr concentrations are generally much lower than that.

For the experiment under Fe-deficient conditions, the concentration of Fe in the Aquil medium was decreased to 0.1 µM total (Fe). Two concentrations of Cr were used in the Cr-treated group: 1 µM Cr was added in the high-Cr group, to maintain the same Cr : Fe ratio as in the Fe-replete experiment, and 0.1 µM Cr was added in the low-Cr group, to achieve a Cr : Fe ratio of 1, which is at the low end of ratios found in the open ocean (GEO-TRACES Intermediate Data Product Group, 2021).

All growth media were adjusted to pH 8.2, which is the present average pH of the surface ocean and then sterilised by filtering through 0.22 µm filters. All growth experiments were conducted in triplicate at a constant temperature of 20 ± 1°C and illuminated with 100 µmol photons m⁻² s⁻¹ on a light-to-dark cycle of 12 h : 12 h.

Since the phytoplankton cells are very small (*c.* 1–1.5 µm), it was difficult to assess cell numbers accurately using a Coulter counter, especially during the early culturing stage when cell numbers were extremely low. Therefore, during the experimental period, the growth of the cultures was monitored regularly using a TECAN Spark® Multimode plate reader to measure the chlorophyll fluorescence (Price & Morel, 1990) and the optical density at 750 nm wavelength (Zhang & Rickaby, 2020). The growth rates were monitored over three generations of subcultures to obtain adapted growth rates and were computed from the following equation:

$$\mu = \frac{\ln N_t - \ln N_0}{t}$$

where N_0 is the previous population size; N_t is the current population size at a time t days after N_0 ; μ is the growth rate.

It has to be noted that only the growth experiments in this part of the study were done with the contrasting Fe conditions. All other experiments, including the measurements of photochemical parameters, metallomes, and proteomes were conducted under Fe-replete condition (1 µM Fe) as the Fe-deficient experiments produced too little biomass for further interrogation.

To investigate the impact of Cr on the photosystem of the phytoplankton, the samples were taken in the third adapted generation when growth rates had stabilised. The maximum photochemical yield of photosystem II (F_v/F_m) and the functional absorption cross-section of photosystem II (σ_{PSII}) in the phytoplankton were measured during the mid-exponential phase, by using the Satlantic FRe System fluorometer (Behrenfeld & Milligan, 2013).

At the end of the experiments, when cultures reached the late exponential phase, cells were harvested via centrifugation at 4816 RCF for 1 h and washed two times with trace-metal clean synthetic ocean water that had been passed through a column packed with chelex 100 resins, and one time with trace-metal clean Tris buffer (20 mM, pH = 8.2), in order to remove the loosely bound metals on cell surfaces (Morel *et al.*, 1979; Zhang *et al.*, 2018b; Wilson *et al.*, 2019). The pellets were preserved for further treatment in preparation for metallome and proteome analysis.

Metallome analysis

For metallome analysis, the harvested cell pellets were digested in quartz-distilled HNO₃ (16 M) and 30% H₂O₂ (v/v). After digestion, the samples were dried on the hot plate and then diluted into 2 ml of 2% HNO₃ before measuring by ICP-MS (Zhang *et al.*, 2018b). The elements measured in the study include W, Ag, Pb, Cd, Ba, Ga, V, As, I, Mo, Br, Se, Co, Ni, Cr, Zr, Ti, Sr, Al, Mn, Zn, Cu, and Fe, and the measurement largely followed our previously reported ICP-MS method (Zhang *et al.*, 2018b). All sample preparation steps for metallome analysis were conducted under trace-metal clean conditions and were undertaken in laminar flow hoods in the Clean Laboratory Suite at the Department of Earth Sciences, University of Oxford. Milli-Q water (18 MΩ cm; Merck Millipore, Burlington, MA, USA) was used where dilution was needed. All centrifuge tubes (Metal-free; VWR, Radnor, PA, USA) and pipette-tips were immersed in 10% quartz distilled HCl for at least 12 h before thoroughly rinsing with 18 MΩ cm water.

Protein extraction

All protein extraction steps were conducted in laminar flow hoods at the Department of Earth Sciences, University of Oxford. The cell pellets were resuspended in the extraction buffer (20 mM Tris-HCl supplement with EDTA-free protease inhibitor (Roche), pH = 8.0) and sonicated six times for 30 s bursts (on ice) with 1-min intervals between sonication (Hielscher UP200S ultrasonic processor, 70% amplitude; Zhang *et al.*, 2018b). The cell lysate was centrifuged at 10 000 *g* at 4°C for 10 min, and the supernatant containing the soluble content of the cytoplasm was passed through a precleaned 0.22 µm PTFE membrane before being subjected to protein digestion for liquid chromatography–tandem mass spectrometry (LC–MS/MS) measurement. The protein concentrations in the samples were measured by Bradford assay (Jones *et al.*, 1989).

Protein sample digestion

Protein samples subjected to proteomic analysis were prepared using a filter-aided sample preparation method (FASP; Wiśniewski, 2017). All steps were performed at the Advanced Proteomics Facility in the Department of Biochemistry, University of Oxford. Vivacon® 500 concentrators (10 kDa cut-off, Sartorius) were used for the preparation. Protein samples (20 µg from each of the triplicate samples of control group and Cr-treated group) were loaded on prewashed FASP filters

and denatured in 8 M freshly made urea in 100 mM triethylammonium bicarbonate (TEAB) solution. The denatured proteins were then reduced with 10 mM tris (2-carboxyethyl) phosphine hydrochloride (TCEP) and alkylated with 50 mM chloroacetamide (CAA) at room temperature in the dark. The samples were then washed several times with 6 M urea in 50 mM TEAB and digested in 0.5 µg endopeptidase (LysC) for 4 h at 37°C and then in 0.5 µg trypsin at 37°C after a four-fold dilution to reduce urea concentration. The samples were collected by centrifugation and acidified by trifluoroacetic acid (TFA) to pH 3 and then cleaned by using in-house made C18 (SUPLECO, Octadecyl C18) columns. The cleaned peptide samples were dried down in a centrifugal evaporator.

Protein mass spectrometry

The peptides were resuspended in 5% formic acid and 5% DMSO prior to mass spectrometry. Peptides were analysed on a Q-Exactive Mass Spectrometer (Thermo Fisher Scientific, Waltham, MA, USA) that was coupled to an Ultimate 3000 ultra-high-performance liquid chromatography (HPLC) system (Thermo Fisher Scientific). The peptides were trapped on a C18 PepMap100 precolumn (300 µm i.d. × 5 mm, 100 Å; Thermo Fisher Scientific) using solvent A (0.1% Formic Acid in water) at a pressure of 500 bar and then separated on an in-house packed analytical column (75 µm i.d. × 50 cm packed with ReproSil-Pur 120 C18-AQ, 1.9 µm, 120 Å, Dr Maisch GmbH) using a linear gradient (length: 65 min, 15–35% solvent B; 0.1% formic acid in acetonitrile; flow rate: 200 nl min⁻¹), which was attached to an EASY-Spray nano-electrospray ion source (Thermo Fisher Scientific). The raw data were acquired on the mass spectrometer in positive-ion mode by data-dependent analysis. Full scan MS spectra were acquired in the Orbitrap (scan range 350–1500 *m/z*, resolution 70 000, AGC target 3e6, maximum injection time 50 ms). After the MS scans, the 10 most intense peaks were selected for HCD fragmentation at 30% of normalised collision energy. HCD MSMS spectra were also acquired in the Orbitrap (resolution 17 500, AGC target 5E4, maximum injection time 120 ms, isolation window 1.5 *m/z*) with the first fixed mass at 180 *m/z*. Dynamic ion exclusion was set to 20 s. Only charge states higher than 1 were considered for fragmentation.

Proteome data processing and statistical analysis

Quantitative data analysis was performed using Progenesis QI for PROTEOMICS software (v.4.1.6675.48614; Nonlinear Dynamics, Newcastle, UK). The Progenesis MASCOT plugin was used to generate a peak list file of MSMS spectra for peptide feature identification, which was searched with MASCOT (v.2.5.1; Matrix Science, London, UK) against the whole UniProt Knowledgebase database (both 'UniProtKB/Swiss-Prot' (reviewed, manually annotated) and 'UniProtKB/TrEMBL' (unreviewed, automatically annotated) databases). Peptide-spectrum match results were exported from MASCOT at default settings (*P* < 0.05) and re-imported into Progenesis, which then calculated relative protein intensities using the top three unique peptides for each protein

(Hi-N method). Progenesis also reported two-condition ANOVA P - and Q -values for each protein using default settings ('raw' protein intensities are multiplied by a run-specific normalisation factor to account for differences in loading, then asinh-transformed before the ANOVA comparison).

Biological function groups

Proteins that had significant change between treatments at 5% false discovery rate (FDR) were considered for further analysis and interpretation. We searched for their Gene Ontology (GO database) and then grouped the proteins according to their functions/pathways. We used the Kyoto Encyclopaedia of Genes and Genomes (KEGG) reference pathways or InterPro to assign tentative biological function where GO terms were not available.

Results

Growth and photochemical parameters in response to Cr addition

Under Fe-replete conditions ($1 \mu\text{M}$ total $[\text{Fe}]$, and 0.3 nM $[\text{Fe}']$ (the free and inorganic Fe in the medium) calculated with an equilibrium speciation model (Visual MINTEQ)), growth rates were significantly increased in the presence of Cr ($10 \mu\text{M l}^{-1}$) over three sub generations compared with the control groups which were cultured in Aquil medium (from $\mu_{\text{control}} = 1.45 \pm 0.03$ to $\mu_{\text{Cr}} = 1.55 \pm 0.01$, $P = 0.004$, Fig. 1). Under Fe-deficient conditions ($0.1 \mu\text{M}$ total $[\text{Fe}]$, $[\text{Fe}'] = 0.03 \text{ nM}$), growth rates were significantly decreased compared with the control group ($\approx 30\% \mu_{\text{control}}$, $P < 0.01$, Fig. 1). Although the growth rates could not be fully restored, supplementing Cr(VI) ($0.1 \mu\text{M l}^{-1}$) into the medium partially rescued the growth of the phytoplankton (an increase of $\approx 17\%$), but such effects were dependent on Cr(VI) and Fe concentrations in the medium (Fig. 1), and the increase in growth rates may reflect 'hormesis' of the phytoplankton in response to the addition of Cr (Calabrese, 2008).

At the exponential phase under Fe-replete conditions, the maximum yield of photochemistry of photosystem II (F_v/F_m) increased significantly in the phytoplankton group in the presence of additional ($10 \mu\text{mol l}^{-1}$) Cr compared with the control Fe-replete group, while the functional absorption cross-section (σ_{PSII}) stayed almost unchanged under these two treatments (Fig. 2).

Cr does not have significant impacts on metallomes of the strain

To determine whether the presence of Cr had any effect on phytoplankton element homeostasis, the whole-cell metallome for the phytoplankton was investigated in the Cr-treated group (Aquil medium + $10 \mu\text{M l}^{-1}$ Cr) and the control group (Aquil medium with no Cr added, Fig. 3). We normalised all trace-metal concentrations to P, as its concentrations in the same biomass were not significantly different in the control and the Cr-

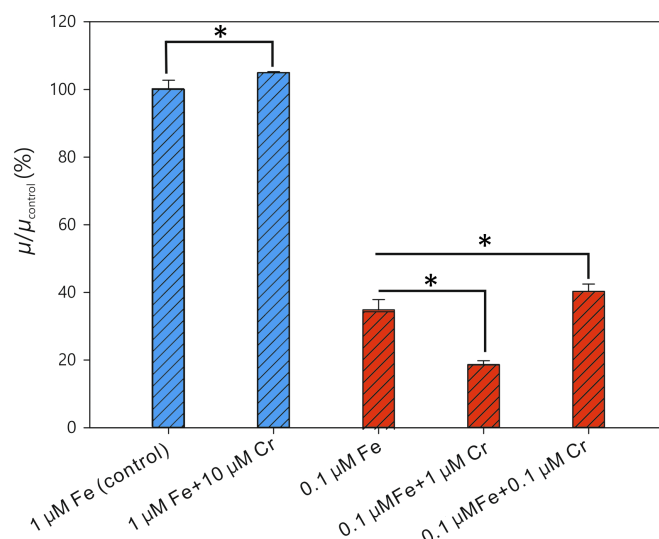


Fig. 1 Under Fe-replete conditions ($1 \mu\text{M l}^{-1}$ Fe, blue bars), $10 \mu\text{M l}^{-1}$ Cr (VI) ($[\text{Cr}] : [\text{Fe}]_{\text{total}} = 10$) stimulated the growth of the phytoplankton. Under Fe-deficient conditions ($0.1 \mu\text{M l}^{-1}$ Fe, red bars), $1 \mu\text{M l}^{-1}$ Cr(VI) ($[\text{Cr}] : [\text{Fe}]_{\text{total}} = 10$) inhibited the growth of the phytoplankton, but $0.1 \mu\text{M l}^{-1}$ Cr(VI) ($[\text{Cr}] : [\text{Fe}]_{\text{total}} = 1$) stimulated the growth of the phytoplankton. *, $P < 0.05$. Error bars: SD.

treated groups ($P = 0.82$). Under Fe-replete conditions, there were no significant changes in cellular concentrations for most trace elements measured in this study, except for Cr and V, whose concentrations increased significantly in groups with added Cr ($P < 0.05$, Fig. 3). An increase in cellular Ni and decrease in Fe, Cu, Pb, Ti, and Ga concentrations, were also hinted in the measurement, but the changes were statistically insignificant (Fig. 3).

Proteomic analysis

To investigate the impact of elevated Cr on phytoplankton protein expression, we conducted proteomic analysis on phytoplankton cultured in normal Aquil medium (control group) and those cultured in Aquil medium with $10 \mu\text{M}$ Cr added (Cr-treated group). We have performed an independent student t -test for the total of 2531 proteins that were identified in the proteomic analysis in the phytoplankton (Supporting Information Table S1). A total of 1752 proteins have their functional homologues identified (69.2%). The remaining third (30.8%) were found to be uncharacterised proteins. The expression of 335 proteins (13.3%) was significantly altered ($P < 0.05$) by the presence of Cr, most of which were associated with secondary metabolism and protein homeostasis (Fig. 4; Table S2). After the application of strict multiple testing corrections (Benjamini & Hochberg, 1995), only 15 proteins were found to be differentially expressed at a 5% FDR-adjusted cut-off (i.e. $q < 0.05$, Table S3). Restricting the analysis to such a low number of proteins precludes further analyses by pathway or biological process enrichment to allow canvassing the differentially expressed proteins and sort them into comprehensive categories. It is suggested that although multiple testing corrections is a useful tool, it could

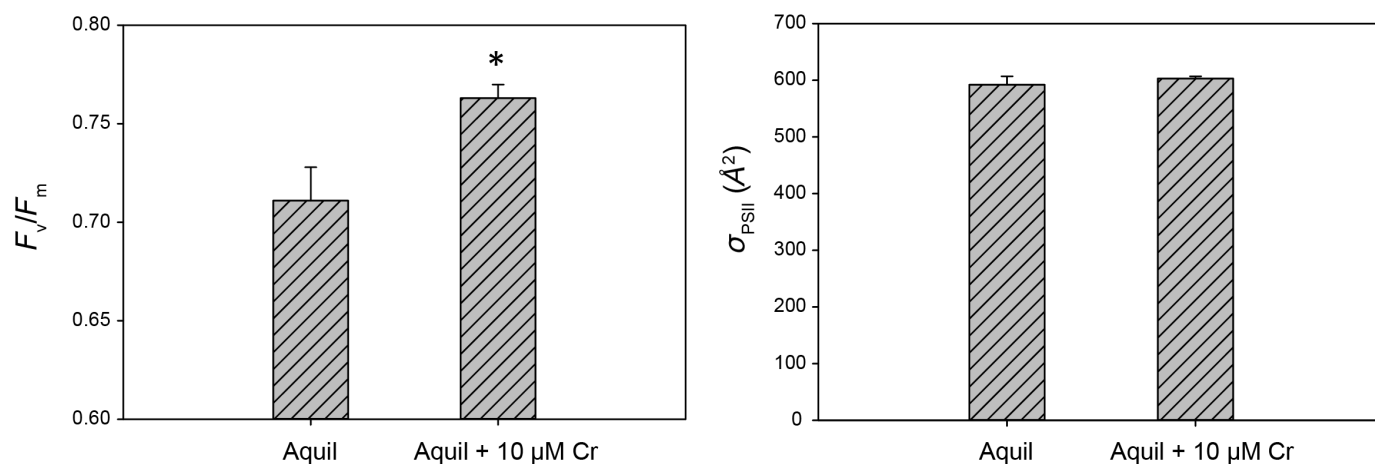


Fig. 2 Compared with the control group (grown in Aquil medium), the photochemical efficiency (F_v/F_m) increased in *Osetreococcus tauri* in the presence of $10 \mu M l^{-1}$ Cr(VI) but the light-harvesting capability (σ_{PSII}) stayed almost unchanged. *, $P < 0.05$. Noted that the scale for the F_v/F_m is from 0.6 to 0.8 in the figure. Error bars: SD of the data.

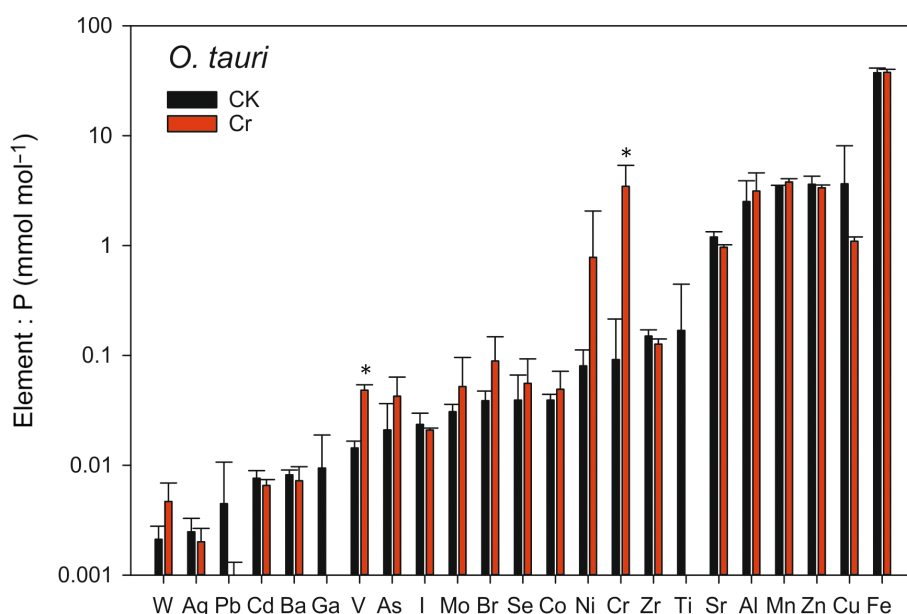


Fig. 3 Whole-cell metallome of *Osetreococcus tauri* in this study. Cr concentration in Cr group (Cr) is significantly higher than that in the control group (CK). Cells in the control group were cultured in Aquil media, and in the Cr group were cultured in Aquil media with supplement of $10 \mu M l^{-1}$ Cr(VI). *, $P < 0.05$. Error bars: SD of the data.

significantly increase false negatives in quantitative proteomics when biological variability is expected to be low and only a small number of replicates ($n = 3$ in this study) are run due to the burdensome cost of undertaking high rates of replication (Pascovici *et al.*, 2016). The anti-conservative P -value histogram in this study indicates Cr treatment truly altered the distribution of proteins in the phytoplankton (Fig. S1). In order to enable a comprehensive understanding of the impact of Cr, we used the uncorrected P -value at 5% FDR as a cut-off, but report associated Q -values and \log_2 fold change as a supplement to our analysis and interpretation (Table S1; Fig. 4). Within the significantly changed proteins ($P < 0.05$) from this analysis, those associated with photosynthesis pathways were all downregulated in the presence of added Cr, but those associated with carbon fixation were upregulated (Fig. 4). Moreover, phosphate and

phosphonate transporters were also found to be downregulated in the presence of Cr (Fig. 4).

Discussion

Photosynthesis and carbon fixation

Although the operation of the Calvin-Benson cycle (C_3 cycle) is believed to be predominant in phytoplankton, the C_4 photosynthetic pathway has also been reported from various marine phytoplankton (Xu *et al.*, 2012). In this study, the key enzymes of the C_3 and C_4 pathways, ribulose-1,5-bisphosphate carboxylase (C_3) and phosphoenol pyruvate carboxylase (C_4), are both found in the proteomic dataset, suggesting the phytoplankton used here may possess both pathways for carbon fixation (Table S1).

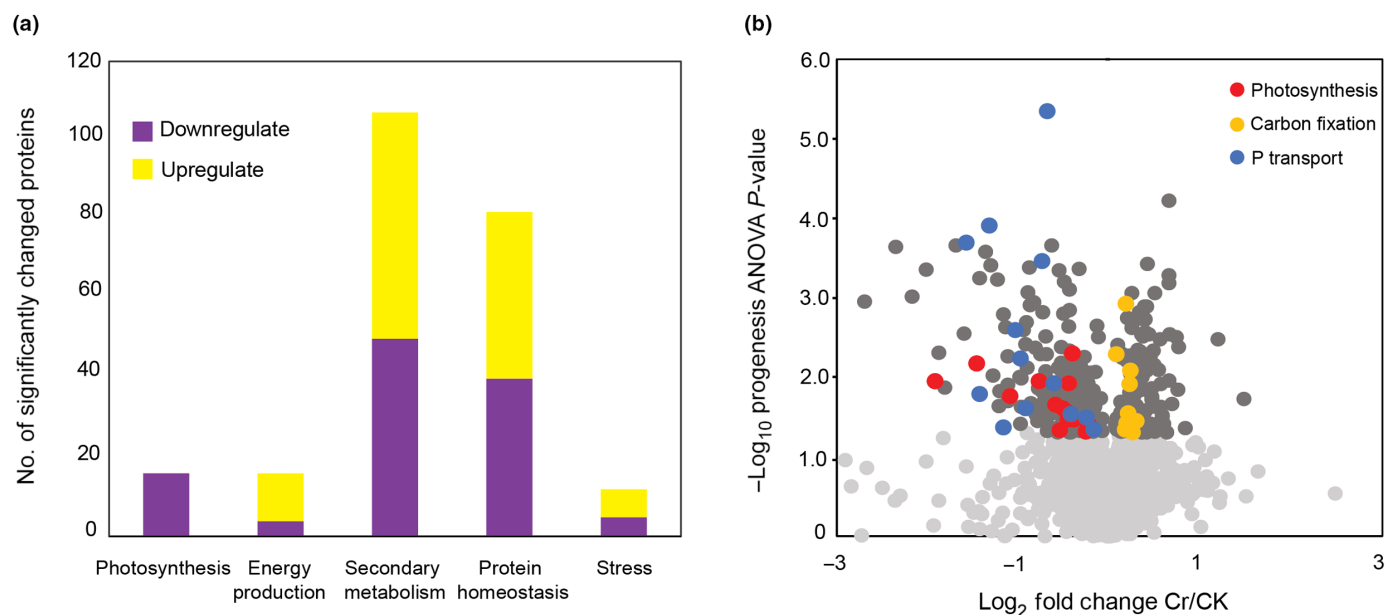


Fig. 4 Proteomic responses of *Osetreococcus tauri* to the addition of Cr(VI). (a) Functional distribution of the number of proteins in *O. tauri* that were significantly impacted by the presence of Cr(VI) in the medium. (b) Volcano plots showing that the expression of proteins related to photosynthesis and phosphate transportation were significantly downregulated, while of those related to carbon fixation were significantly upregulated.

The photosynthesis pathway appears to have been impacted by the presence of elevated Cr in this study. Although many photosynthesis-related proteins were significantly downregulated in the group treated with Cr (Fig. 4), the photosynthesis process in the phytoplankton showed a higher efficiency in this group. During exponential growth phase, the maximum yield of photochemistry of photosystem II (F_v/F_m) increased significantly in the group treated with Cr ($P < 0.05$), while there was no significant difference in the F_0 compared with the control after the dark treatment before the measurement ($P = 0.27$). The functional absorption cross-section (σ_{PSII}) remained unchanged (Fig. 2) in both groups. F_v/F_m is an often-used measure of photosynthetic efficiency (Falkowski *et al.*, 1992; Boyd & Abraham, 2001), and it has been suggested that submaximal values of F_v/F_m could indicate physiological stress in phytoplankton (Falkowski *et al.*, 1992). Moreover, based on our proteomic analysis, the photosynthetic processes and the carbon assimilation processes seemed to become decoupled with higher Cr concentrations. With decreased expression of photosynthetic-related proteins, the expression level of proteins related to the carbon assimilation process increased significantly (Fig. 4). In phytoplankton, carbon fixation is just one of the multiple sinks for ATP and reductant generated from photosynthesis. The relative fraction of photosynthate dedicated to carbon fixation can be determined by several factors, including the demand for new carbon products relative to ATP and reductant, the ATP and reductant yield of parallel carbon metabolisms, the requirements for carbon storage, and the differences in the production and demand ratios for energy (Behrenfeld *et al.*, 2008). Here, we hypothesise that the specific metabolic processes that were influenced by Cr and acted to decouple carbon fixation from photosynthesis in the phytoplankton might be related to the intracellular Cr-binding sites.

Previous studies have endeavoured to separate out Cr-binding proteins from mammalian cells, but until now, the only available candidate for Cr use *in vivo* was the low molecular weight Cr-binding complex (LMWCr), and the structure or sequence of these complexes are still largely unknown (Feng *et al.*, 2003; Peterson *et al.*, 2008). We tried to trace the Cr-binding protein extracted from the phytoplankton in this study using protein separation by HPLC and separated protein fractions measured by ICP-MS (Methods S1). In this approach, Cr-binding proteins were found to always coelute with Fe-binding proteins (Fig. S2). Considering the strong similarities between Cr(III) and Fe(III) in terms of their ionic radii and other atomic properties, such coelution of the Fe and Cr protein was not surprising, as Cr(VI) is known to readily reduced to Cr(III) once it enters into cells (Macfie *et al.*, 2010; Viti *et al.*, 2014). Although we have not identified Cr-binding proteins in *Osetreococcus*, our previous work confirmed that most proteins in the Cr-rich fraction from different species of phytoplankton contained iron-sulphur clusters (Table S4). In human cells, a competition between Cr and Fe for Fe-binding sites has long been established (Harris, 1977). Evidence indicates that Cr has a great affinity for transferrin, and it has been suggested that this major iron transport protein in the blood also transports Cr *in vivo* (Harris, 1977; Deng *et al.*, 2015; Levina *et al.*, 2016). Moreover, many previous studies suggested that iron-sulphur clusters are primary intracellular targets associated with the toxicity of various metals, including copper (Macomber & Imlay, 2009), cobalt (Ranquet *et al.*, 2007), silver, mercury, cadmium, and zinc (Xu & Imlay, 2012). Although pure Cr-binding protein isolation has not yet been achieved, from the HPLC-ICP-MS data here (Fig. S2; Table S4), a potential valid explanation is that Cr invaded some Fe-binding sites in the proteins, with the

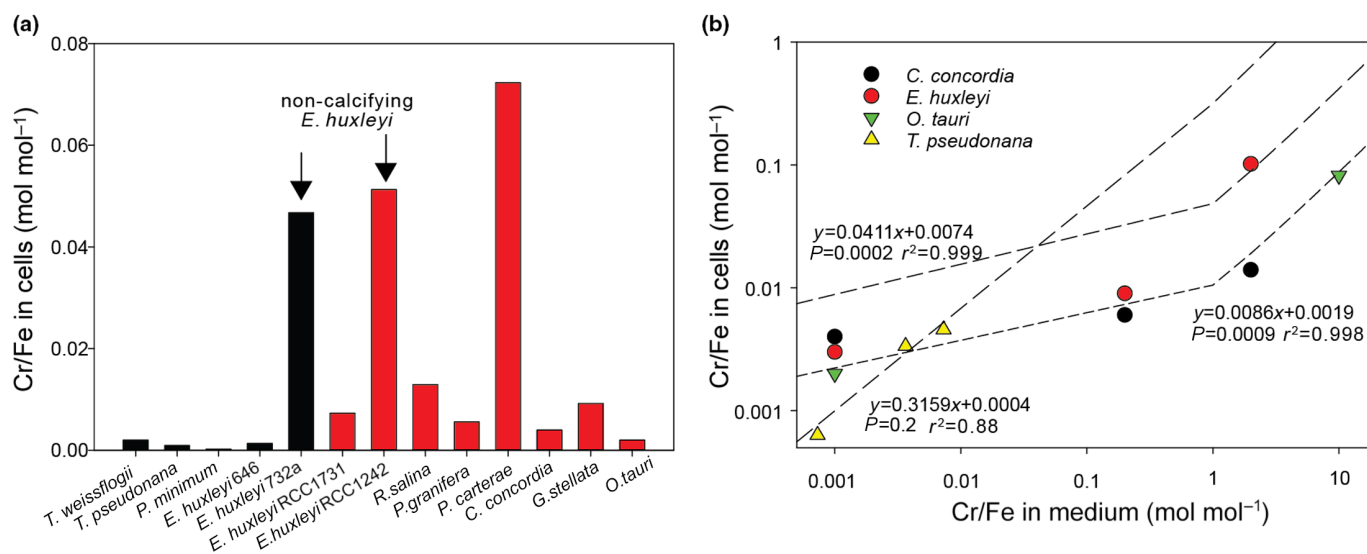


Fig. 5 Variations of [Cr] : [Fe] ratios in different phytoplankton. (a) Cr : Fe in different phytoplankton cells under Fe-replete conditions (total [Fe] > 1000 nM and [Cr(VI)] < 5 nM in medium). Black bars: Cr data are from (Semeniuk *et al.*, 2016) and Fe data are from Ho *et al.* (2003) and Imura *et al.* (2016). Red bars: measured in this study. (b) Cr : Fe in cells vs Cr : Fe in the medium. For comparison between different studies, total Fe concentration in the medium was used in the calculation. Data for *Clethrha Concordia* and *Emiliania huxleyi* are from (Wilson *et al.*, 2019), for *Thalassiosira weissflogii* are from (Semeniuk *et al.*, 2016), and for *Osetreococcus tauri* are from this study. Lines indicate the linear relationships between Cr : Fe in cells and Cr : Fe in growth medium. Noted that same growth medium (Aquil) was used in different studies.

main targets being iron–sulphur clusters in the phytoplankton. In the photosynthetic electron transport chains, iron–sulphur clusters not only serve as the terminal electron-accepting cofactors in photosystem I (PS I), but also act as electron transfer cofactors in the cytochrome *b₆f* complex and in soluble ferredoxin (Jin *et al.*, 2008; Liu *et al.*, 2014). Therefore, it is not surprising that partial Cr substitution on these Fe–S clusters may have a large influence on the efficiency of the photosystem in phytoplankton. In the intracellular environment, the species of Cr may change due to reactions with different cellular components. Although Cr(VI) would ultimately reduce to Cr(III), short-lived Cr(VI) and Cr(IV) have been detected in previous studies, and it has been suggested that some of the short-lived Cr(V) would be oxidised to Cr(VI) intracellularly. Therefore, Cr(VI) may also react with Fe–S clusters. Since Cr(VI) has a higher redox potential than Fe(III), it may be that the Cr induced a higher energy output through the electron transfer processes in the photosystem to support the carbon assimilation process, and this is one possible explanation for the decoupling of the photosynthetic and carbon fixation from the proteomic data, but it requires further study to fully decipher the mechanisms involved. We note that even if this is the case, Cr will only replace a very small proportion of Fe in these proteins, since the decrease in Fe concentration was not statistically significant (mmol Fe per mol P, Fig. 3) in the presence of Cr under Fe-replete conditions. The whole-cell Cr : Fe was < 0.1 mol mol⁻¹ in Cr(VI) treated group (Fig. 5). Moreover, it has been established that < 10% whole-cell Cr would be present in the cytosol fraction in Chlorophytes; > 90% of Cr would be bound with metal-rich granules associated with the membrane fraction (Wilson *et al.*, 2019). Thus, Cr : Fe ratio in proteins would be even lower than 0.1 mol mol⁻¹.

Phosphate/phosphite/phosphonate transporters

Previous study by Semeniuk *et al.* (2016) suggests that Cr(VI) would reduce to Cr(III) before entering the cells of some phytoplankton species including diatoms and one coccolithophore *Emiliania huxleyi*. Such reduction and accumulation of Cr(III) was not found in other nondiatom species, suggesting Cr(VI) was the major species that entered the cells in those phytoplankton (Semeniuk *et al.*, 2016). The phytoplankton investigated in this study was neither a diatom nor a coccolithophore, and therefore, considering that Cr species were not determined during transmembrane uptake processes in our study, it is more likely that Cr entered the cells as Cr(VI) before its intracellular reduction into Cr(III), as suggested by numerous other studies (Viti *et al.*, 2014; Zhang *et al.*, 2019a,b; Marković *et al.*, 2022).

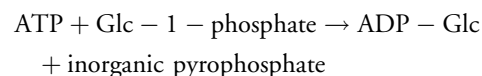
The significant decrease in phosphate/phosphite/phosphonate transporters found in the group treated with Cr may be linked to the mechanisms for Cr uptake and transport processes. Although it was suggested that Cr mainly enters the cell via sulphate channels (Riedel, 1985; Cheung & Gu, 2007; Viti *et al.*, 2014; Zhang *et al.*, 2021), in some microorganisms, it can be transported through nonspecific anion carriers that can also transport phosphate and nitrate (Cervantes, 2001). In the plant *Arabidopsis thaliana*, there is evidence showing that phosphate can relieve Cr toxicity by interfering with chromate uptake (López-Bucio *et al.*, 2014; Wu *et al.*, 2018), but sulphate and nitrate cannot decrease Cr(VI) uptake by the plant, suggesting that phosphate transporters might be essential for Cr(VI) uptake and transport in plants. In this study, both prokaryotic and eukaryotic types of phosphate ABC transporters were found to decrease in the Cr (VI) treated group, indicating that not only the cellular phosphate uptake process was downregulated by the presence of Cr

(VI), but phosphate transport processes into the plastids may also have been impacted (Zheng *et al.*, 2013; Locher, 2016; Tables S1–S3). Moreover, *Pho* regulon, the genes that are positively regulated in response to limiting external inorganic phosphorus (Pi) levels, were also found to be downregulated in response to Cr(VI) treatment (Table S1), which could be a result of potential Cr toxicity that disrupted the cell sensing for potential P requirement (Vuppada *et al.*, 2018). Therefore, it is likely that the intracellular Pi content may decrease under Cr treatment, although this did not affect the whole-cell P content in our study, as cellular phosphorus contents were not significantly decreased under Cr treatment. Phosphorus was mostly complexed in the organic forms intracellularly and the inorganic Pi forms a small proportion of the intracellular P that in total only constitutes < 1/3 of total P in phytoplankton (Zhang *et al.*, 2018b). Nevertheless, since Pi is an essential component for many important metabolic pathways in phytoplankton, the impacts of Cr on its transport and cycling processes may affect many crucial biological functions, such as energy metabolism, starch biosynthesis, and carbon fixation.

Starch biosynthesis in the phytoplankton

The strain studied here can accumulate a single starch granule at the chloroplast centre (Fig. S3). The starch produced by the phytoplankton may provide a stored source of energy and carbon surplus during nutrient-limiting conditions, which can be an advantageous feature for the species. Indeed, previous studies showed that many organisms, including bacteria, plants, and yeast, can accumulate carbon and energy by producing polysaccharides as reserve compounds, to cope with starvation conditions in various environments (Ballicora *et al.*, 2003; Yao *et al.*, 2012; Van Lis *et al.*, 2017). The synthesis of storage polysaccharides in cell is maximal when cellular carbon and energy are in excess (Stark *et al.*, 1992; Zeeman *et al.*, 2010). Therefore, starch production is linked with carbon assimilation in the cell, which was suggested to have increased in Cr-treated group in this study, according to the increased expression of proteins in the phytoplankton.

The biochemical pathway of polysaccharide biosynthesis in bacteria and plants, namely glycogen and starch respectively, was suggested to involve the use of ADP-Glucose pyrophosphorylase (Ballicora *et al.*, 2003), which catalyses the following reaction (Espada, 1962):



Sequences of ADP-Glucose pyrophosphorylase (Glucose-1-phosphate adenylyltransferase) were found in the proteomic analysis (Table S1), indicating that the phytoplankton studied here use the ADP-Glc pathway for synthesising starch in cells. The expression level of ADP-Glucose pyrophosphorylase in the phytoplankton was not impacted by the presence of Cr in the medium (Table S1), but the change in its activator/inhibitor level in response to Cr treatment could affect the enzyme activity. The

main activator and inhibitor for ADP-Glucose pyrophosphorylase of cyanobacteria, green algae, and higher plants, are found to be 3-phosphoglycerate (3-PGA) and Pi, respectively (Charrng *et al.*, 1992; Iglesias & Preiss, 1992). In this study, 3-PGA production was found to have increased, likely as a response to a significant increase in ribulose biphosphate-carboxylase/oxygenase (RubisCO) expression (Table S1), which catalyses its production. Moreover, a potential decrease in phosphorus content intracellularly was indicated by a significant decrease in the expression of many phosphate-transporting proteins in the cell treated with Cr ($P < 0.05$; Fig. 4). Therefore, it is likely that there was an increase in starch production in the presence of Cr due to an increase in the ratio of 3-PGA : Pi in cells.

Relationship of Cr and Fe in marine phytoplankton

In the modern ocean, the surface biological uptake and remineralisation at depth, or biological pump, has been suggested to be responsible for the nutrient-like depth profiles of both dissolved Fe (Sunda, 1988; Moore *et al.*, 2013) and Cr (Jeandel & Minster, 1987; Scheiderich *et al.*, 2015) in seawater. Although we only conducted a detailed investigation on one species in our study, here we extend our analysis to compare Cr : Fe in multiple marine phytoplankton in response to Cr : Fe in the medium at Fe-replete conditions, to investigate how the availability of Fe and Cr interact to be possibly beneficial to algae in natural seawater. When [Cr] and [Fe] were comparable to average surface seawater concentrations (i.e. both at nM levels, but $[\text{Fe}]_{\text{total}} > 1 \mu\text{M}$, Table S5), the Cr : Fe ratio was found to be between 0.0002 and 0.07 mol mol⁻¹ in different marine phytoplankton, with the data from the strain in this study within this range (Fig. 5a; Semeniuk *et al.*, 2016; Zhang *et al.*, 2018b; Wilson *et al.*, 2019; Zhang & Rickaby, 2020). A feature to note is that noncalcifying *E. huxleyi* have a much higher cellular Cr : Fe ratio than the calcifying *E. huxleyi*. Such contrasting features between calcifying and noncalcifying strains were also reported for Tl, and it was suggested that the secretion process of the coccoliths might be an efflux pathway for some trace metals (Zhang & Rickaby, 2020). When the Cr concentration is elevated, the Cr : Fe in the phytoplankton increased with an increase in Cr : Fe in the medium (due to an increase in Cr concentrations with consistent Fe concentration in the medium), but mostly with very low slopes (< 0.1 when Cr : Fe < 1 (mol mol⁻¹)), indicating the cells effectively discriminate against uptake of Cr from the media and have a much higher selectivity or effective preference for incorporation of Fe relative to Cr by at least a factor of 10 (Fig. 5b). The slopes were different for various phytoplankton species, and the data from this study fit well with those for *Clethrha concordia*, which is a chlorophyte more closely related to the strain studied here (Fig. 5b). The variation in the slopes suggests a difference in Cr accumulation/discrimination ability in the phytoplankton species, which may be responsible for the potential difference in Cr content and utilisation in phytoplankton (Fig. 5a). A previous study investigating the impact of Cr was conducted under Fe-replete conditions (Wilson *et al.*, 2019), but here we discovered that the beneficial and toxic effects of Cr(VI)

on phytoplankton also depend on the availability of Fe. Under Fe-replete conditions in this study (1 μM total [Fe]), 10 μM Cr (VI) can stimulate the growth of the phytoplankton (Cr : Fe = 10). However, in the experiments where the Fe concentration was sufficiently low to limit the growth of the phytoplankton (0.1 μM total [Fe]), a significantly lower Cr(VI) concentration (0.1 μM) was required to stimulate the growth of the phytoplankton (Cr : Fe = 1, Fig. 1). At low [Fe] concentrations (0.1 μM), Cr(VI) became toxic to the phytoplankton at a concentration of 1 μM , but Cr(VI) concentrations in seawater seldom reach such a level. Dissolved Fe concentrations in the open ocean are typically at the nM and pM level (Kuma *et al.*, 1996; Liu & Millero, 2002; Klar *et al.*, 2018), and the average Cr(VI) concentration determined in the open ocean is *c.* 2.4 nM (Goring-Harford *et al.*, 2018), may be well below concentrations that are toxic to phytoplankton but with the potential to be at comparable levels to Fe and then beneficial to some of the phytoplankton species. Nevertheless, the comparisons and conclusions made in this study were based on experimental data, which may not fully represent natural conditions, due to uncertainties with regard to variations in phytoplankton species and natural ligand complexes that may affect both Cr and Fe bioavailability. Therefore, such hypothesis is fertile avenue for future studies.

Our study indicates that there is a delicate balance between Cr stimulation of growth and toxicity, and such effects depend on Fe availability. If too much Cr(VI) is present in the medium, it would cause toxicity effects in phytoplankton. However, once a delicate amount of Cr(VI) is added to the medium, it might be able to substitute for Fe(III) in some of the proteins and induce beneficial effects for phytoplankton once it is reduced to Cr(III) in the intracellular environment. Although there are no previous data on phytoplankton, an early study by (Barceló *et al.*, 1993) also demonstrated the beneficial influence of Cr(III) on the chloroplast ultrastructure in Fe-deficient plants. Since Cr : Fe ratios are found to be different in different phytoplankton (Fig. 5), the delicate balance between Cr toxicity and potential benefit may also depend on the species of phytoplankton and the selectivity of their transporter system. Further study needs to be done to isolate and identify the Cr-binding proteins to test the hypothesis raised in this study. However, if Cr is indeed competing and partially substituting for Fe in phytoplankton and improving photosynthetic efficiency, it might have great implications in the marine environment, where Fe concentrations are known to be limiting (Schlitzer *et al.*, 2018).

Acknowledgements

This project has received funding from the European Research Council (ERC) under the European Union's Horizon 2020 research and innovation programme (APPELS project, grant agreement no. 681746). Qiong Zhang acknowledges funding support from Southern Marine Science and Engineering Guangdong Laboratory Independent Research grant SML2021SP204 and CORE. CORE is a joint research centre for ocean research between QNLM and HKUST. We are grateful to Phil Holdship

for support with analyses by ICP-MS, and to Dr Sabrina Libratori for support with proteomic analysis. Electron microscopy was performed in the Sir William Dunn School EM facility at the University of Oxford, and we are grateful to Dr Errin Johnson for sample preparation and advice. We are grateful to the Discovery Proteomics Facility in the Target Discovery Institute, University of Oxford, for use of their copy of Progenesis to analyse the data.

Competing interests

None declared.

Author contributions

QZ designed and performed the experiments, analysed the data, and wrote the manuscript. PDC provided technical support for proteomic data analysis. EMB contributed to methodology and manuscript editing. SSH and SM provided support for methodology establishment. REMR contributed to data interpretation and manuscript editing.

ORCID

El Mahdi Bendif  <https://orcid.org/0000-0002-2508-4787>
Philip D. Charles  <https://orcid.org/0000-0001-5278-5354>
Shabaz Mohammad  <https://orcid.org/0000-0003-2640-9560>
Rosalind E. M. Rickaby  <https://orcid.org/0000-0002-6095-8419>
Qiong Zhang  <https://orcid.org/0000-0002-9007-8025>

Data availability

The data that supports the findings of this study are available in the [Supporting Information](#) of this article.

References

- Aharchaoui I, Rosabal M, Liu F, Battaglia E, Vignati DAL, Fortin C. 2017. Bioaccumulation and subcellular partitioning of Cr(III) and Cr(VI) in the freshwater green alga *Chlamydomonas reinhardtii*. *Aquatic Toxicology* **182**: 49–57.
- Ballicora MA, Iglesias AA, Preiss J. 2003. ADP-glucose pyrophosphorylase, a regulatory enzyme for bacterial glycogen synthesis. *Microbiology and Molecular Biology Reviews* **67**: 213–225.
- Barceló J, Poschenrieder C, Dolores Vázquez M, Gunsé B. 1993. Beneficial and toxic effects of chromium in plants: solution culture, pot and field studies. *Studies in Environmental Science* **55**: 147–171.
- Beerling DJ, Kantzas EP, Lomas MR, Wade P, Eufrazio RM, Renforth P, Sarkar B, Andrews MG, James RH, Pearce CR *et al.* 2020. Potential for large-scale CO₂ removal via enhanced rock weathering with croplands. *Nature* **583**: 242–248.
- Behrenfeld MJ, Halsey KH, Milligan AJ. 2008. Evolved physiological responses of phytoplankton to their integrated growth environment. *Philosophical Transactions of the Royal Society, B: Biological Sciences* **363**: 2687–2703.
- Behrenfeld MJ, Milligan AJ. 2013. Photophysiological expressions of iron stress in phytoplankton. *Annual Review of Marine Science* **5**: 217–246.
- Belevich TA, Milyutina IA, Abyzova GA, Troitsky AV. 2021. The pico-sized Mamiellophyceae and a novel Bathycoccus clade from the summer plankton of

- Russian Arctic Seas and adjacent waters. *FEMS Microbiology Ecology* 97: faa251.
- Benjamini Y, Hochberg Y. 1995. Controlling the false discovery rate: a practical and powerful approach to multiple testing. *Journal of the Royal Statistical Society Series B (Statistical Methodology)* 57: 289–300.
- Boyd PW, Abraham ER. 2001. Iron-mediated changes in phytoplankton photosynthetic competence during SOIREE. *Deep-Sea Research Part II: Topical Studies in Oceanography* 48: 11–22.
- Calabrese EJ. 2008. Hormesis: why it is important to toxicology and toxicologists. *Environmental Toxicology and Chemistry* 27: 1451–1474.
- Cervantes C. 2001. Interactions of chromium with microorganisms and plants. *FEMS Microbiology Reviews* 25: 335–347.
- Chang Y, Kakefuda G, Iglesias AA, Buikema WJ, Preiss J. 1992. Molecular cloning and expression of the gene encoding ADP-glucose pyrophosphorylase from the cyanobacterium *Anabaena* sp. strain PCC 7120. *Plant Molecular Biology* 20: 37–47.
- Cheung KH, Gu J-D. 2007. Mechanism of hexavalent chromium detoxification by microorganisms and bioremediation application potential: a review. *International Biodeterioration & Biodegradation* 59: 8–15.
- Deng G, Wu K, Cruce AA, Bowman MK, Vincent JB. 2015. Binding of trivalent chromium to serum transferrin is sufficiently rapid to be physiologically relevant. *Journal of Inorganic Biochemistry* 143: 48–55.
- Espada J. 1962. Enzymic synthesis of adenosine diphosphate glucose from glucose 1-phosphate and adenosine triphosphate. *The Journal of Biological Chemistry* 237: 3577–3581.
- Falkowski PG, Greene RM, Geider RJ. 1992. Physiological limitations on phytoplankton productivity in the ocean. *Oceanography* 5: 84–91.
- Feng W, Li B, Liu J, Chai Z, Zhang P, Gao Y, Zhao J. 2003. Study of chromium-containing proteins in subcellular fractions of rat liver by enriched stable isotopic tracer technique and gel filtration chromatography. *Analytical and Bioanalytical Chemistry* 375: 363–368.
- Flipkens G, Blust R, Town RM. 2021. Deriving Nickel (Ni(II)) and Chromium (Cr(III)) based environmentally safe olivine guidelines for coastal enhanced silicate weathering. *Environmental Science and Technology* 55: 12362–12371.
- GEOTRACES Intermediate Data Product Group. 2021. The GEOTRACES Intermediate Data Product 2021 (IDP2021). *NERC EDS British Oceanographic Data Centre* NOC.
- Goring-Harford HJ, Klar JK, Pearce CR, Connelly DP, Achterberg EP, James RH. 2018. Behaviour of chromium isotopes in the eastern sub-tropical Atlantic Oxygen Minimum Zone. *Geochimica et Cosmochimica Acta* 236: 41–59.
- Harris DC. 1977. Different metal-binding properties of the two sites of human transferrin. *Biochemistry* 16: 560–564.
- Ho T, Quigg A, Zoe V, Milligan AJ, Falkowski PG, Morel MM. 2003. The elemental composition of some marine phytoplankton. *Journal of Phycology* 39: 1145–1159.
- Iglesias AA, Preiss J. 1992. Bacterial glycogen and plant starch biosynthesis. *Biochemical Education* 20: 196–203.
- Imura Y, Sasai K, Ya IS, Yoshimura E. 2016. Citrate as a possible iron-pooling substance in the marine diatom *Thalassiosira pseudonana*. *Marine Biology* 163: 138.
- Jeandel C, Minster JF. 1987. Chromium behavior in the ocean: global versus regional processes. *Global Biogeochemical Cycles* 1: 131–154.
- Jin Z, Heinicke M, Krebs C, Shen G, Golbeck JH, Bryant DA. 2008. Biogenesis of iron-sulfur clusters in photosystem I: Holo-NfuA from the cyanobacterium *Synechococcus* sp. PCC 7002 rapidly and efficiently transfers [4Fe-4S] clusters to apo-PsaC *in vitro*. *Journal of Biological Chemistry* 283: 28426–28435.
- Jones CG, Daniel Hare J, Compton SJ. 1989. Measuring plant protein with the Bradford assay. *Journal of Chemical Ecology* 15: 979–992.
- Klar JK, Schlosser C, Milton JA, Woodward EMS, Lacan F, Parkinson IJ, Achterberg EP, James RH. 2018. Sources of dissolved iron to oxygen minimum zone waters on the Senegalese continental margin in the tropical North Atlantic Ocean: Insights from iron isotopes. *Geochimica et Cosmochimica Acta* 236: 60–78.
- Kuma K, Nishioka J, Matsunaga K. 1996. Controls on iron(III) hydroxide solubility in seawater: the influence of pH and natural organic chelators. *Limnology and Oceanography* 41: 396–407.
- Levina A, Pham THN, Lay PA. 2016. Binding of chromium (III) to transferrin could be involved in detoxification of dietary chromium (III) rather than transport of an essential trace element. *Angewandte Chemie, International Edition* 55: 8104–8107.
- Liu J, Chakraborty S, Hosseinzadeh P, Yu Y, Tian S, Petrik I, Bhagi A, Lu Y. 2014. Metalloproteins containing cytochrome, iron-sulfur, or copper redox centers. *Chemical Reviews* 114: 4366–4469.
- Liu X, Millero FJ. 2002. The solubility of iron in seawater. *Marine Chemistry* 77: 43–54.
- Locher KP. 2016. Mechanistic diversity in ATP-binding cassette (ABC) transporters. *Nature Structural and Molecular Biology* 23: 487–493.
- López-Bucio J, Hernández-Madrigrá F, Cervantes C, Ortiz-Castro R, Carreón-Abud Y, Martínez-Trujillo M. 2014. Phosphate relieves chromium toxicity in *Arabidopsis thaliana* plants by interfering with chromate uptake. *Biometals* 27: 363–370.
- Macfie A, Hagan E, Zhitkovich A. 2010. Mechanism of DNA-protein cross-linking by chromium. *Chemical Research in Toxicology* 23: 341–347.
- Macomber L, Imlay JA. 2009. The iron-sulfur clusters of dehydratases are primary intracellular targets of copper toxicity. *Proceedings of the National Academy of Sciences, USA* 106: 8344–8349.
- Marković S, Levstek L, Žigon D, Ščančar J, Milačič R. 2022. Speciation and bio-imaging of chromium in taraxacum officinale using HPLC post-column ID-ICP-MS, high resolution MS and laser ablation ICP-MS techniques. *Frontiers in Chemistry* 10: 863387.
- Moore CM, Mills MM, Arrigo KR, Berman-Frank I, Bopp L, Boyd PW, Galbraith ED, Geider RJ, Guieu C, Jaccard SL *et al.* 2013. Processes and patterns of oceanic nutrient limitation. *Nature Geoscience* 6: 701–710.
- Morel FMM, Rueter JG, Anderson DM, Guillard RRL. 1979. Aquil: a chemically defined phytoplankton culture medium for trace metal studies. *Journal of Phycology* 15: 135–141.
- Pascovici D, Handler DCL, Wu JX, Haynes PA. 2016. Multiple testing corrections in quantitative proteomics: a useful but blunt tool. *Proteomics* 16: 2448–2453.
- Peterson RL, Banker KJ, Garcia TY, Works CF. 2008. Isolation of a novel chromium (III) binding protein from bovine liver tissue after chromium (VI) exposure. *Journal of Inorganic Biochemistry* 102: 833–841.
- Pfeiffer WC, Fiszman M, Drude de Lacerda L, van Weerelt M, Carbonell N. 1982. Chromium in water, suspended particles, sediments and biota in the Irajá River estuary. *Environmental Pollution. Series B: Chemical and Physical* 4: 193–205.
- Price NM, Morel FMM. 1990. Cadmium and cobalt substitution for zinc in a marine diatom. *Nature* 344: 658–660.
- Ranquet C, Ollagnier-de-Choudens S, Loiseau L, Barras F, Fontcave M. 2007. Cobalt stress in *Escherichia coli*: the effect on the iron-sulfur proteins. *Journal of Biological Chemistry* 282: 30442–30451.
- Richard FC, Bourg ACM. 1991. Aqueous geochemistry of chromium: a review. *Water Research* 25: 807–816.
- Riedel GF. 1985. The relationship between chromium (VI) uptake, sulfate uptake, and chromium (VI) toxicity in the estuarine diatom *Thalassiosira pseudonana*. *Aquatic Toxicology* 7: 191–204.
- Rudnick RL, Gao S. 2003. The composition of the continental crust. In: Holland HD, Turekian KK, eds. *Treatise on geochemistry*. Oxford, UK: Pergamon, 1–64.
- Scheiderich K, Amini M, Holmden C, Francois R. 2015. Global variability of chromium isotopes in seawater demonstrated by Pacific, Atlantic, and Arctic ocean samples. *Earth and Planetary Science Letters* 423: 87–97.
- Schlitzer R, Anderson RF, Dodas EM, Lohan M, Geibert W, Tagliabue A, Bowie A, Jeandel C, Maldonado MT, Landing WM *et al.* 2018. The GEOTRACES intermediate data product 2017. *Chemical Geology* 493: 210–223.
- Semeniuk DM, Maldonado MT, Jaccard SL. 2016. Chromium uptake and adsorption in marine phytoplankton – implications for the marine chromium cycle. *Geochimica et Cosmochimica Acta* 184: 41–54.
- Stark DM, Timmerman KP, Barry GF, Preiss J, Kishoret GM. 1992. Regulation of the amount of starch in plant tissues by ADP glucose pyrophosphorylase. *Science* 258: 287–292.
- Sunda W, Price N, Morel F. 2005. Trace metal ion buffers and their use in culture studies. In: *Algal culturing techniques*. Burlington, MA, USA: Academic Press, 35–63.

- Sunda WG. 1988. Trace metal interactions with marine phytoplankton. *Biological Oceanography* 6: 411–442.
- Taylor LL, Quirk J, Thorley RMS, Kharecha PA, Hansen J, Ridgwell A, Lomas MR, Banwart SA, Beerling DJ. 2016. Enhanced weathering strategies for stabilizing climate and averting ocean acidification. *Nature Climate Change* 6: 402–406.
- Van Lis R, Poppek M, Couté Y, Kosta A, Drapier D, Nitschke W, Atteia A. 2017. Concerted up-regulation of aldehyde/alcohol dehydrogenase (ADHE) and starch in *Chlamydomonas reinhardtii* increases survival under dark anoxia. *Journal of Biological Chemistry* 292: 2395–2410.
- Viti C, Marchi E, Decorosi F, Giovannetti L. 2014. Molecular mechanisms of Cr (VI) resistance in bacteria and fungi. *FEMS Microbiology Reviews* 38: 633–659.
- Vuppada RK, Hansen CR, Strickland KAP, Kelly KM, McCleary WR. 2018. Phosphate signaling through alternate conformations of the PstSCAB phosphate transporter. *BMC Microbiology* 18: 1–9.
- Wilson W, Zhang Q, Rickaby REM. 2019. Susceptibility of algae to Cr toxicity reveals contrasting metal management strategies. *Limnology and Oceanography* 64: 2271–2282.
- Wiśniewski JR. 2017. Filter-aided sample preparation: the versatile and efficient method for proteomic analysis. *Methods in Enzymology* 585: 15–27.
- Wu S, Hu Y, Zhang X, Sun Y, Wu Z, Li T, Lv J, Li J, Zhang J, Zheng L *et al.* 2018. Chromium detoxification in arbuscular mycorrhizal symbiosis mediated by sulfur uptake and metabolism. *Environmental and Experimental Botany* 147: 43–52.
- Xu FF, Imlay JA. 2012. Silver (I), mercury (II), cadmium (II), and zinc (II) target exposed enzymic iron-sulfur clusters when they toxify *Escherichia coli*. *Applied and Environmental Microbiology* 78: 3614–3621.
- Xu J, Fan X, Zhang X, Xu D, Mou S, Cao S, Zheng Z, Miao J, Ye N. 2012. Evidence of coexistence of C₃ and C₄ photosynthetic pathways in a green-tide-forming alga, *Ulva prolifera*. *PLoS ONE* 7: 1–10.
- Yao C, Ai J, Cao X, Xue S, Zhang W. 2012. Enhancing starch production of a marine green microalga *Tetraselmis subcordiformis* through nutrient limitation. *Bioresource Technology* 118: 438–444.
- Yung CCM, Redondo ER, Sanchez F, Yau S, Piganeau G. 2022. Diversity and evolution of Mamiellophyceae: early-diverging phytoplanktonic green algae containing many cosmopolitan species. *Journal of Marine Science and Engineering* 10: 240.
- Zeeman SC, Kossmann J, Smith AM. 2010. Starch: its metabolism, evolution, and biotechnological modification in plants. *Annual Review of Plant Biology* 61: 209–234.
- Zhang B, Duan G, Fang Y, Deng X, Yin Y, Huang K. 2021. Selenium (IV) alleviates chromium (VI)-induced toxicity in the green alga *Chlamydomonas reinhardtii*. *Environmental Pollution* 272: 116407.
- Zhang Q, Amor K, Galer SJG, Thompson I, Porcelli D. 2018a. Variations of stable isotope fractionation during bacterial chromium reduction processes and their implications. *Chemical Geology* 481: 155–164.
- Zhang Q, Amor K, Galer SJG, Thompson I, Porcelli D. 2019a. Using stable isotope fractionation factors to identify Cr(VI) reduction pathways: Metal-mineral-microbe interactions. *Water Research* 151: 98–109.
- Zhang Q, Bendif EM, Zhou Y, Nevado B, Shafiee R, Rickaby REM. 2022. Declining metal availability in the Mesozoic seawater reflected in phytoplankton succession. *Nature Geoscience* 15: 932–941.
- Zhang Q, Rickaby REM. 2020. Interactions of thallium with marine phytoplankton. *Geochimica et Cosmochimica Acta* 276: 1–13.
- Zhang Q, Snow JT, Holdship P, Price D, Watson P, Rickaby REM. 2018b. Direct measurement of multi-elements in high matrix samples with a flow injection ICP-MS: application to the extended: *Emiliania huxleyi* redfield ratio. *Journal of Analytical Atomic Spectrometry* 33: 1196–1208.
- Zhang Q, Song Y, Amor K, Huang WE, Porcelli D, Thompson I. 2019b. Monitoring Cr toxicity and remediation processes – combining a whole-cell bioreporter and Cr isotope techniques. *Water Research* 153: 295–303.
- Zheng WH, Västermark Å, Shlykov MA, Reddy V, Sun EI, Saier MH. 2013. Evolutionary relationships of ATP-Binding Cassette (ABC) uptake porters. *BMC Microbiology* 13: 98.

Supporting Information

Additional Supporting Information may be found online in the Supporting Information section at the end of the article.

Fig. S1 *P*-value histogram of all proteins identified in this study.

Fig. S2 Cr and Fe abundance profiles measured by ICP-MS after size exclusion chromatographic fractionation of the Cr-treated phytoplankton cytosol fraction by HPLC.

Fig. S3 TEM image of the *Osetreococcus tauri* strain in this study.

Methods S1 Metalloprotein chromatography using HPLC and ICP-MS.

Table S1 Proteins identified in the chlorophyte *Osetreococcus tauri* in this study for both control (CK) and Cr-treated groups (CR).

Table S2 Descriptions and functions for *Osetreococcus tauri* proteins that are significantly expressed under Cr treatment ($P < 0.05$).

Table S3 Proteins that are found to be differentially expressed at 5% FDR-adjusted cut-off after applying strict multiple testing corrections.

Table S4 Proteins identified in the fraction in which Cr and Fe signal from ICP-MS was overlapped in phytoplankton (*Emiliania huxleyi* (RCC1242) and *Clethra Concordia* (RCC1)).

Table S5 Chemical species present in the growth medium.

Please note: Wiley is not responsible for the content or functionality of any Supporting Information supplied by the authors. Any queries (other than missing material) should be directed to the *New Phytologist* Central Office.